

AUTOMATED REMOVAL OF OVERSHOOT ARTEFACT FROM IMAGES

Naomi Harte and Anil Kokaram

Dept. Electronic and Electrical Engineering, Trinity College Dublin,
 Dublin 2, Ireland
 phone: + (353) 6081580, fax: + (353) 6772442, email: nharte@tcd.ie
 web: www.sigmedia.tv

ABSTRACT

This paper presents a simple but robust technique for overshoot removal from video sequences. The artefact of overshoot is modelled as a filter which distorts the step response of edges within the affected image. By detecting strong vertical edges in an image and measuring the distorted step response, an equalising filter can be designed to restore the step response closer to the ideal response and hence minimise the overshoot visible in the picture. The algorithm is presented along with results for both real archived images and images with known distortions. This allows performance in terms of Peak Signal to Noise Ratio to be assessed. The performance is shown to be good both quantitatively and qualitatively. The limitation of the approach is shown to be the lack of preservation of finer detail in some cases. Performance could be enhanced by first assigning areas of fine detail in the image which should not be processed. Application to video sequences is also considered where the equaliser update is weighted between the current and previous frame to reduce flicker artefacts.

1. INTRODUCTION

Signal processing methods to automate the restoration of image sequences has become an area of strong interest in recent years. The increased market for archived video resources has lead to a concerted effort to rectify the artefacts frequently encountered in archives due to, for example, physical degradation or chemical decomposition of the original material. Typical defects include Dirt and Sparkle, Film Tear, Colour Fading and Dropout [1]. Automated methods of restoration are clearly advantageous considering the sheer amount of data potentially involved.

The work presented in this paper is focussed on one particular artefact - that of overshoot. Overshoot artefacts are visible on abrupt transitions (vertical edges) in affected video. This phenomena can be caused by problems such as rapid cut-off bandwidth limitation or excessive aperture correction. For example, in telecine transfer when a sharp dark-to-light transition occurs, badly-tuned circuitry can produce an overshoot in step response rather than a smooth step transition. This results in an apparent bright edge or halo along the right vertical edge. An example of an image with overshoot is shown in Figure 1 on the left, along with the corresponding measured step response on the right. The solid blue line indicates the measured response and the red dashed line the ideal or desired step response.

The terms of echo and overshoot are frequently mentioned together in relation to image artefacts involving image shadows in the frame. However, for the purposes of this work, it should be clear that these two artefacts are consid-

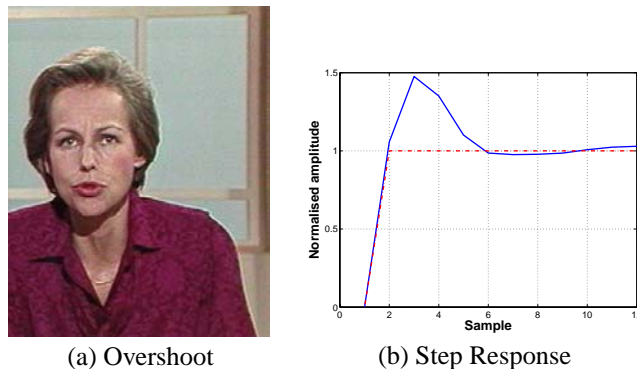


Figure 1: Image displaying overshoot (a) on left shoulder of newscaster and measured step response (b). Image courtesy of INA. Christine Ockrent. A2. 30/12/82

ered as separate problems with different causes despite their (sometimes) similar manifestation. Much research has been conducted into problems associated with echo due to delay transmissions where a test signal may [2] or may not [3] [4] be available to help design an equaliser. Overshoot, in contrast, is not well addressed in published research. Hence this paper presents initial work on the design of an automated overshoot removal algorithm.

2. OVERSHOOT REMOVAL

The overall approach taken is to measure the distorted step response from affected edges in an image and design a filter to remove the overshoot from the response. The algorithm has three main elements:

- Edge detection and step measurement
- Equaliser design
- Masking

These will be discussed more fully in the following sections.

2.1 Edge Detection

Edge detection is performed as the first step in order to isolate strong vertical edges in the affected picture. This is done by firstly using a Difference of Gaussian (DoG) filter and then thresholding the gradient at zero crossings [5]. The resulting edges are searched for strong continuous vertical, or near vertical, edges that would typically indicate an object with overshoot occurring along the right hand edge. This is an important step as reliable isolation of the edges is critical for a correct subsequent measurement of the distorted response. The response from each continuous edge must be tested to as-

certain whether the edge detected is actually a strong vertical transition as not all the edges isolated in the edge detection will yield a true step. The stability of the response is also tested. All suitable edges are measured to calculate the average step response. This is then averaged and normalised to give a classic $0 \rightarrow 1$ step transition in the steady-state. This yields the actual step response $s(n)$ and the corresponding target step response $s'(n)$ can be assigned. If an insufficient number of steps are measured from the image to give an accurate response, the image is left unaltered.

The description of the target step response as ideal is an area that may warrant more investigation. For the current work, the ideal response is taken as the $0 \rightarrow 1$ step transition. It is felt however that some small amount of overshoot may actually be favourably perceived by the viewer. This would be better investigated if the response was measured at a sub-pixel level, allowing for greater accuracy in the representation of the step.

2.2 Equalisation

Having obtained a measure of the distorted step response, the aim is to design an equalising filter to convert this distorted step into the desired step response. The Steiglitz McBride Iteration [6] can be used to find the coefficients of an equalising IIR filter which given a particular input can produce a specified output. In this application, the system input is $s(n)$ and the desired output is $s'(n)$. The iteration minimises the square error between the actual and desired output. The resulting filter has impulse response $h(n)$ with equivalent system transfer function $H(z)$ as:

$$H(z) = \frac{b(1) + b(2)z^{-1} + \dots + b(M+1)z^{-M}}{a(1) + a(2)z^{-1} + \dots + a(N+1)z^{-N}} \quad (1)$$

where M and N are the number of zeros and poles respectively in the system response. For this work, an all pole system with between 7 and 9 poles have proven sufficient in most cases.

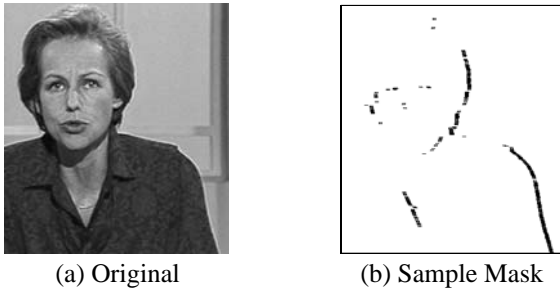


Figure 2: Original image with corresponding mask for pixel replacement

The original image I is then filtered to yield I' . Rather than use this image as output however, as many details in the overall picture quality will become blurred in the filtering process, only pixels in the region of the original strong vertical edges are replaced. The original edges from the initial step in the algorithm are dilated to produce a masking matrix M_{filt} to isolate pixels that are replaced. A corresponding matrix M_{orig} is derived as the inverse of M_{filt} . Hence the output

image I_{out} can be constructed as:

$$I_{out} = M_{orig}I + M_{filt}I' \quad (2)$$

This is demonstrated in Figure 2(b) which shows the mask for the image in (a). Only the shaded pixels in (b) will be replaced in (a). The importance of the masking step is discussed further in the results section.

2.3 Extension to Sequences

To this point, the work has considered overshoot removal in terms of the artefact present in a single image. Most of the affected material for restoration is actually in the form of video sequences where it is vital to consider the performance of the algorithm across successive frames. Hence this work has also explored the processing of image sequences affected by overshoot. As will be discussed in the results section, adaptation of the equaliser across frames rather than independent processing of frames has been found to be important in terms of perceived quality of the restored sequence.

3. PERFORMANCE EVALUATION

This section examines the performance of the overshoot removal algorithm as presented. Performance is assessed in two ways; by introducing a known distortion to an image and comparing Peak Signal to Noise Ratio (PSNR) before and after processing by the overshoot removal module, and by visual inspection of performance for real images.

3.1 Image with Known Distortion

A simple filter with a pair of poles at $0.1370 \pm 0.7932i$ was constructed to add overshoot into test images. By then using the overshoot removal algorithm to restore the image, a quantitative comparison with the original unaffected image is possible. Two test images were used. The first is a simple test pattern with rectangles varying in gray level. This is shown in Figure 3(a). For this image, overshoot addition is restricted to vertical lines but the variation in transition levels demonstrated the performance over a good range of edges. The second image in Figure 3(e) is a real image with a variety of non-vertical edges to test the overshoot removal.

Comparison was done by calculating the Peak Signal to Noise Ratio between the original image and that with introduced overshoot, and between the original image and that with overshoot removed. The PSNR is a commonly used measure of quality of reconstruction in image compression. It can be expressed in terms of the mean squared error (MSE), which for two $r \times c$ monochrome images I and K , where one image is a noisy approximation of the other, is defined as

$$MSE = \frac{1}{rc} \sum_{i=0}^{r-1} \sum_{j=0}^{c-1} \|I(i, j) - K(i, j)\|^2 \quad (3)$$

The PSNR can then be defined in terms of the MSE as:

$$PSNR = 20 \log_{10} \left(\frac{255}{\sqrt{MSE}} \right) \quad (4)$$

where in this case 255 is the maximum pixel value in the original image I .

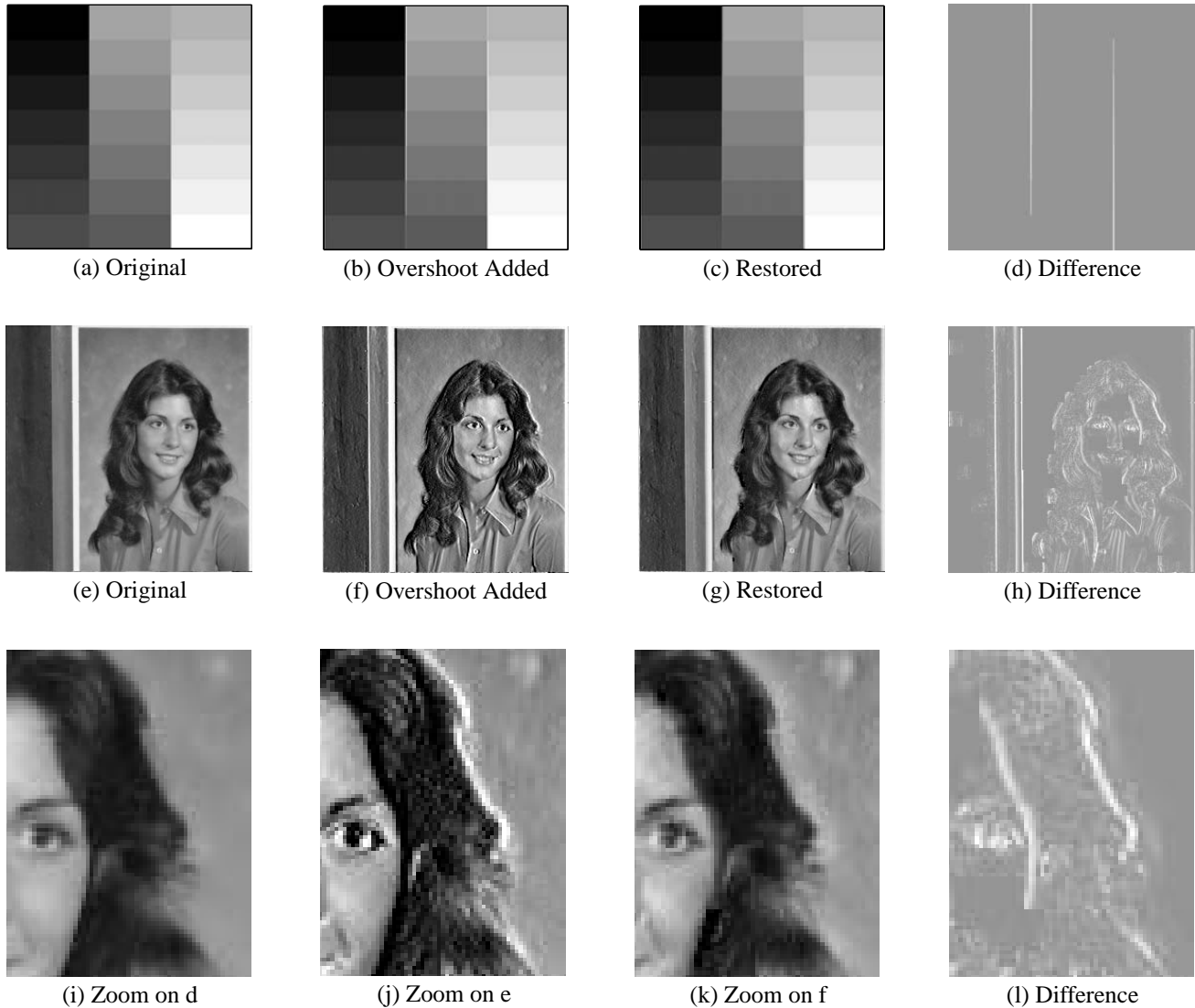


Figure 3: Test patterns with inserted overshoot and restored image after overshoot removal. Frame difference is shown on the far right in each case.

Original Image	PSNR with Overshoot	PSNR after Overshoot Removal
Figure 3 (a)	29.69dB	32.06dB
Figure 3 (d)	19.19dB	23.36dB

Table 1: PSNR values for Overshoot removal.

The PSNR values in Table [1] correspond with the images displayed in Figure 3(a) and (e). In the case of (a), a 2.5 *dB* improvement in PSNR is achieved after removal of the overshoot. The overshoot here is restricted to exact vertical edges by nature of the image content. This demonstrates the overshoot can reliably be measured and equalised in situations of this type. The difference image in (d) represents the frame difference between the image with added overshoot (b) and the restored image in (c). It shows that the overshoot at the transition between the darkest levels (bottom left) and lightest levels (top right) is not detected.

A 4 *dB* improvement in PSNR is achieved for the second

test image shown in Figure 3(e). Overall the PSNR values are lower as expected due to the greater relative distortion introduced. This is apparent in (f). The overall quality of the restored image in (g) is clearly better. A closer zoom on detail in this image in Figure 3(i-k) indicates that the reconstruction of the image in areas of overshoot is good though some tones are not correctly restored.

It is worth noting that for both these images, a distortion has been added to the entire image to achieve an addition of overshoot. Hence in real images, where the overshoot is only present on edges, the output picture quality will be better. The masking process described is specifically introduced to ensure this. The equaliser, by design, will smooth edges in the picture and this would result in significant blurring of all edges if applied to the entire image. The mask dilates the original vertical edges to define where pixels should be replaced. This helps to preserve detail in the image. Notwithstanding the masking process, the removal has still worked best in areas of strong vertical edges where detail is coarse

relative to the picture scale. Many images will have finer detail close to affected edges and hence the masking process cannot protect these regions. This suggests that performance could be enhanced by a pre-processing step whereby areas of the image not to be processed could be assigned by the user.

3.2 Real Images

For images with existing overshoot, only a qualitative analysis is possible. The image shown in Figure 1 was processed using the described algorithm and results are shown in Figure 4. Note that overall for colour images, it has been found to be better to only process the luminance or Y component and then reconstruct the image in the relevant colour space. Figure 4(b) shows a zoom of detail along the arm of the presenter where strong overshoot is apparent in the original in (a). In regions where the edge is closer to vertical, the overshoot removal performs well. Closer to the top of the shoulder, the removal is not as complete. This is because the algorithm performs best in regions of overshoot on continuous strong vertical lines.

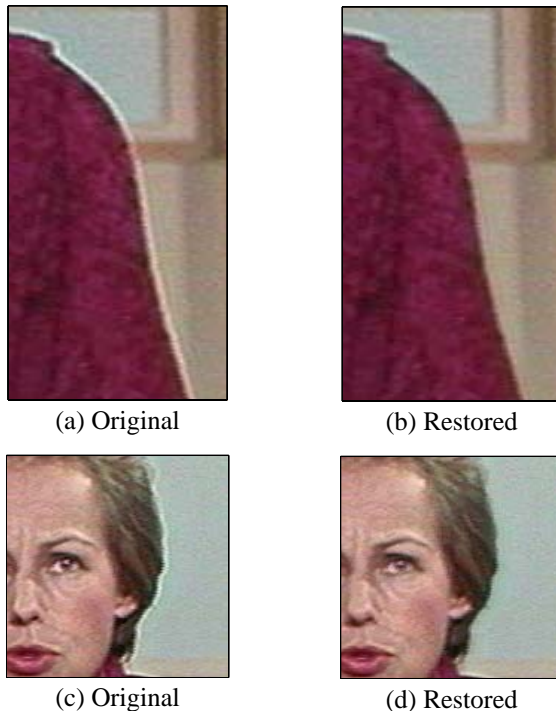


Figure 4: Clip before and after overshoot removal.

Figure 4(c) shows detail from the head region in the same image. The overshoot removal again performs well though some blurring of detail in the face is apparent in (d). This is due in part to the accuracy of the mask M_{filr} derived from the dilated edges. It is important to minimise any noise in the edges which will be grown in the dilation process. Furthermore, the edge along the nose in the face is detected as a vertical edge and the algorithm does not attempt to consider detail in the region of the edge. This is another case where a user stage designating such areas as not to be processed may be advantageous. Figure 5 shows the results for an image where overshoot is apparent along the edge of a set of steps. The removal is better along the vertical edge of the step as

the overshoot is not completely removed where it is present along the diagonal edge.

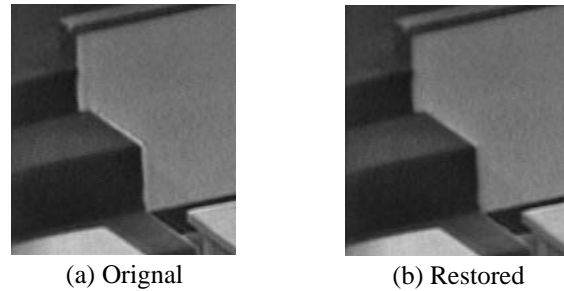


Figure 5: Additional example

3.3 Image sequences

The performance of the algorithm on image sequences has also been tested. When frames were processed as independent images and played back, there can be strong flicker in the region of overshoot where pixels have been replaced. This problem is exacerbated when the object with overshoot is moving. Ideally, the motion of the object the edge belongs too could be tracked to ensure equivalent pixels were always replaced around the object. However, this would greatly increase the complexity of the algorithm. Experimentation with a range of sequences concluded that the optimal flicker reduction was obtained when the distorted step measurement was gradually updated across frames. The update is based on a weighted combination of the average distorted step from the current frame $s(n)$ and that from the previous frame $s(n-1)$, using the classic averaging filter as:

$$s_w(n) = \alpha s(n) + (1 - \alpha)s(n-1) \quad (5)$$

where α values of between .7 and .5 have proven optimal.

The results of this approach are analysed in Figure 6. At the top of this figure, 4 non-consecutive frames from a 150-frame sequence are shown. There is only limited motion of the newscaster in the sequence. The surface plot in (a) shows the measured step response taken along the isolated edges in each frame. The plot in (b) shows the same information when the step response is averaged across the current and previous frame as defined in Eq. 5. Here a value of $\alpha = 0.7$ has been used. It can be seen that the variation in step response has been reduced and hence the equaliser varies less from frame to frame. This has been sufficient to reduce the amount of flicker between frames. Another method of reducing flicker has been to merge the mask from the current and previous frame. This can be very effective in sequences such as this one where motion is limited and the mask is moving slowly. Testing with more sequences is required to establish the best overall approach.

4. DISCUSSION

This paper has presented a simple algorithm for overshoot removal from images. The algorithm has been shown to improve the PSNR in images where a known distortion introducing overshoot has been added. The performance for real images with overshoot has also been shown to be reliable when the images being processed have strong vertical edges

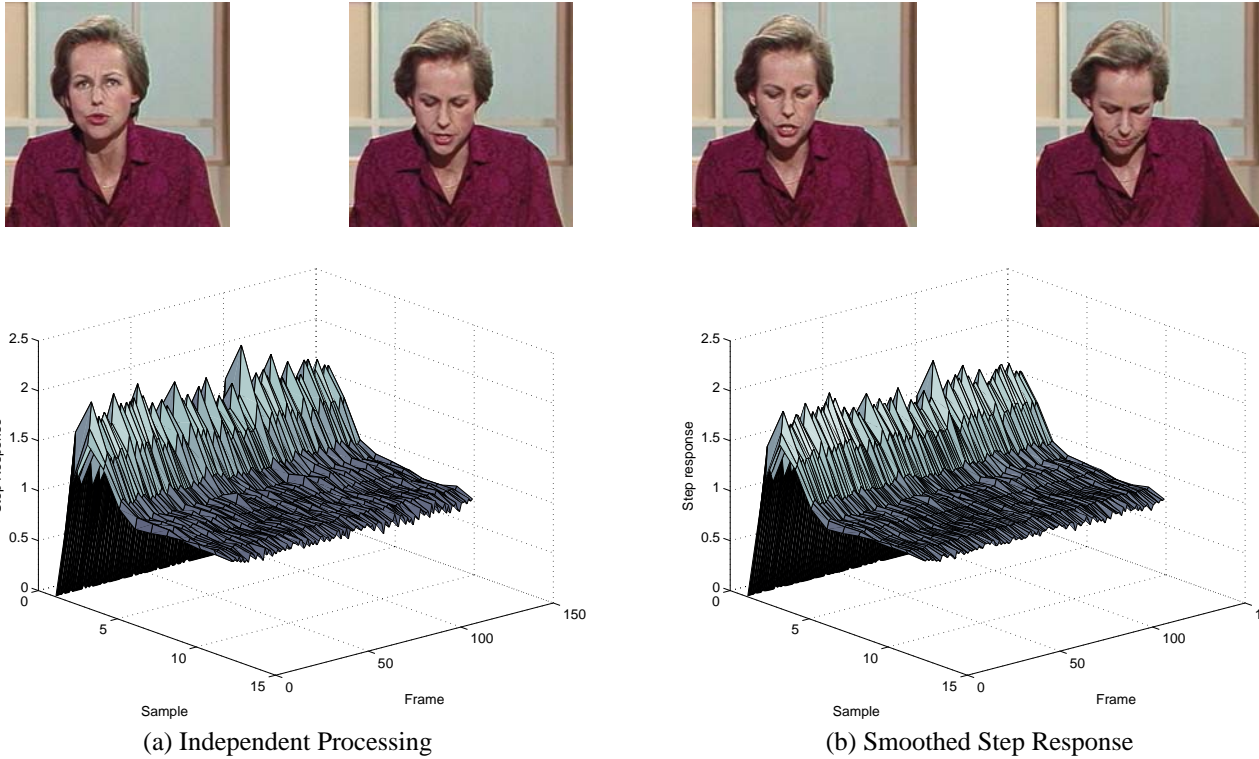


Figure 6: The 4 frames above are sample frames across the 150 frame sequence. The evolution of step response across the 150 frames is shown in (a) and (b). In (a), the step response is measured independently for each frame. In (b), the step is weighted as described in Eq. 5 with $\alpha = 0.7$

without too much fine detail. The processing is fully automated though some parameter adjustment is necessary for new sequences, such as the gradient threshold for edge detection and the dilation for masking. Initial work on video sequences has considered an adaptive scheme across successive frames to address problems with flicker. Both an averaging of step response and merging of masks from the current and previous frame have addressed the problem for sequences with limited motion. Work is ongoing to increase overall robustness and improve performance for sequences.

REFERENCES

- [1] Kokaram, A.C., "On missing data treatment for degraded video and film archives: a survey and a new Bayesian approach." *IEEE Transactions on Image Processing*, Volume 13, Issue 3, March 2004, pp. 397-415 .
- [2] D'Alto, V.; Cremonesi, A.; Casnati, A.; Dassiè, L.; Dal Poz, S., "Video deghosting using adaptive echo-detecting IIR filters." *IEEE Transactions on Consumer Electronics*, Vol 39, Issue 4, pp 754-764.
- [3] Lei, Z. , Appelhans, P. , Schroder, H., "Image processing techniques for blind TV ghost cancellation", *Proc. ICASSP 1997*, Vol 4, pp. 2561-2564.
- [4] Appelhans, P., Schroder, H., "Ghost cancelling for stationary and mobile television." *IEEE Transactions on Consumer Electronics*, Aug 1995, Vol 41, Issue 3, pp. 472-475.
- [5] Marr, D., "Vision: a computational investigation into the human representation and processing of visual information," W.H. Freeman, 1982.
- [6] Steiglitz, K., & L.E. McBride, "A Technique for the Identification of Linear Systems." *IEEE Trans. Automatic Control*, Vol. AC-10 (1965), pp. 461-464.